Gene Expression, Vol. 11, pp. 23–34
Printed in the USA.

1052-2166/03 $20.00 + .00

www.cognizantcommunication.com

Absolute Quantitation of Normal and ROS-Induced Patterns of Gene Expression: An In Vivo Real-Time PCR Study in Mice

MARÍA-JOSÉ PRIETO-ÁLAMO, JUAN-MANUEL CABRERA-LUQUE, AND CARMEN PUEYO[1]

Departamento de Bioquímica y Biología Molecular, Campus de Rabanales edificio C-6, Carretera Madrid-Cádiz Km 396-a, Universidad de Córdoba, 14071-Córdoba, Spain

Most studies using real-time PCR are taken semiquantitatively and assume a steady level of expression for the so-called housekeeping genes. By absolute real-time PCR we demonstrate that the transcript amounts of two of the most popular internal controls (coding GAPDH and β-actin) fluctuate dramatically across diverse mouse or human tissues. This raises the question about the inaccuracy of these genes as quantitative references in tissue-specific mRNA profiling. Target genes chosen for absolute real-time PCR analysis are involved in DNA repair, regulation of gene expression, and oxidative stress response. Hence, they code for 8-oxoG-DNA glycosylase/AP-lyase, major AP-endonuclease, and heme oxygenase-1. Quantitations reported: i) determine mouse-to-mouse variability in basal gene expression, ii) establish organ- and embryo-associated differences in mouse, iii) compare mouse and human tissue-specific profiles, iv) examine the time course (30–240 min) expression in liver and lung of mice treated with paraquat (superoxide generator) at 30 mg kg^{-1} (one half LD_{50} value), and v) explore the utility of absolute real-time PCR in field studies with genetically diverse mice. We conclusively establish that real-time PCR is a highly sensitive and reproducible technique for absolute quantitation of transcript levels in vivo and propose its use to quantitate gene expression modulation under mild physiological exposures and for field epidemiological studies.

Absolute real-time PCR In vivo gene expression Mice *GAPDH* *ACTB* *OGG1* *APE1* *HO-1* Paraquat Oxidative stress

THE mouse has become an indispensable and versatile model organism for human studies. Recently, much has been learned about mammalian gene expression through large-scale analyses with cDNA arrays. However, this method offers only an estimate of relative message levels and does not allow reliable quantitative analysis on a large scale of specimens. Quantitation of expression profiles of key genes in mammals is of great interest to assess fundamental processes of development, genetics, behavior, and disease. For investigations aimed at quantitative analysis, the sensitivity of the PCR-based methods will hardly be reached by any other technique.

The use of reverse transcription real-time PCR technique for quantitation of gene expression has dramatically increased over the past few years. Among others, the technique has been applied to complex in vivo systems involving mammalian tissues and organs to confirm microarray results (34) and/or to provide new biomarkers for epidemiological studies (17, 21). Most real-time PCR studies make relative comparisons of mRNA levels between different samples. In relative quantitation, a gene not expected to exhibit expression variation between samples is used as reference to normalize the RT-PCR data. Nevertheless, it cannot be taken for granted that the so-called housekeeping genes will maintain a steady level of expression in all biological contexts and under all experi-

Accepted October 16, 2002.
[1]Address correspondence to Carmen Pueyo, Departamento de Bioquímica y Biología Molecular, Campus de Rabanales edificio C-6, Carretera Madrid-Cádiz Km 396-a, Universidad de Córdoba, 14071-Córdoba, Spain. Tel: +34 957 218695; Fax: +34 957 218688; E-mail: bb1pucuc@uco.es

mental circumstances. In fact, expression of putative stable housekeeping genes may vary as much as that of the target gene (13,17,41).

Ionizing radiation, chemical mutagens and carcinogens, and normal cellular metabolism form reactive oxygen species (ROS). ROS are involved in the process of carcinogenesis and other human pathogenesis (49). Virtually all aerobic organisms have evolved a complex repertoire, often redundant, of antioxidant defenses to mitigate the damaging effect of ROS on DNA, proteins, and lipids (9).

A major site of ROS attack is at the C8 position of guanine to produce 8-oxoguanine, which is a mutagenic and carcinogenic oxidative DNA damage. In mammalian cells this genotoxic lesion is removed from the genome through the 8-oxoG-DNA glycosylase/AP-lyase activities coded for by the *OGG1* gene (6,26,37). Apurinic/apyrimidinic (AP) sites are a common type of DNA lesion. The major mammalian AP endonuclease (the product of *APE1*; also designated as *REF1* or *APEX*) is a multifunctional protein with a role on a wide variety of important cellular functions. Therefore, APE1 is a critical component of the DNA base excision repair pathway; it is involved in oxidative DNA damage repair and also represents a novel redox factor of signal transduction processes that regulate eukaryotic gene expression (14). Recent data indicate that in human OGG1 and APE1 proteins might cooperate with each other in the process of base excision repair for 8-oxoguanine in double-stranded DNA (19,40).

Heme oxygenase (HO) is the rate-limiting enzymatic activity in heme degradation, catalyzing the cleavage of the heme ring to form ferrous iron, carbon monoxide, and biliverdin. To date, three isoforms (HO-1, HO-2, and HO-3) have been identified. Of the two major variants, HO-1 (also known as heat-shock protein HSP32) is a stress-response enzyme while HO-2 is virtually uninducible. Although the prototypical HO-1 inducer is the substrate heme, HO-1 can also be stimulated by a variety of nonheme products including UV irradiation, endotoxin, heavy metals, and oxidants such as hydrogen peroxide (33). The housekeeping genes encoding for glyceraldehyde-3-phosphate-dehydrogenase (*GAPDH*) and β-actin (*ACTB*) are most commonly used to normalize patterns of gene expression (42).

We have used real-time PCR for absolute quantitation of the transcript levels of five genes (hereafter named *OGG1, APE1, HO-1, GAPDH*, and *ACTB*) in samples from different murine (m) and human (h) organs. As outlined above, the genes analyzed were chosen on the basis of their implication in key cellular events such as DNA repair, regulation of gene expression, and oxidative stress response, or for being advocated as quantitative references in most expression analyses. Experimental evidence reported here might serve to overcome putative concerns over the sensitivity, reproducibility, and validity of absolute expression data generated by real-time PCR. Moreover, our results emphasize the requirement for rigorous absolute quantitation when using real-time PCR for in vivo expression studies in mammals. Ultimately, data presented may contribute to further understanding of the biological significance of the mammalian *OGG1, APE-1*, and *HO-1* genes, thus facilitating the studies aimed to prove the relation between oxidative damage and human diseases.

MATERIALS AND METHODS

Animals and Treatments

Male BALB/c mice (*Mus musculus*), 7 weeks of age (24–26 g), were obtained from Charles River Laboratories (Spain). Following a 3-day acclimation period animals were divided into groups of three subjects. Treated animals were injected IP with paraquat (PQ) at a single dose of 30 mg kg^{-1} body weight dissolved in normal saline. Control animals received a single IP injection of saline solution. Mice were sacrificed at 30, 60, 120, and 240 min after injection. Basal expression levels were determined in noninjected mice. Animals were individually killed by cervical dislocation. The liver, spleen, kidney, testis, heart, lung, and brain were removed, in that order, and immediately frozen in liquid nitrogen. Care was taken to ensure that a maximum of 10 min elapsed between time of death and harvest of the last organ. Mice were handled according to the norms stipulated by the European Community. The investigation was performed after approval by the Ethical Committee of the University of Córdoba (Spain).

Field Study

Algerian mice (*Mus spretus*) were captured with live Sherman traps in autumn of 2001 at five different sampling areas. They included: i) Gerena (a nonpolluted area upstream from the Aznalcóllar dam), ii) Mina de Aznalcóllar (the mine tailings dam), and iii) Aznalcázar (AZN), Cangrejo grande (CG), and Brazo de la Torre (BDT), three sampling areas along the Guardiamar river course [see geographical location in (38)]. The mice were then taken alive to the nearby laboratory at the Doñana Biological Reserve, where their sex, weight, and size were determined. Immediately after, male and female animals of similar size and weighing around 10 g were sacrificed and dissected. The livers were removed and taken frozen in liquid nitrogen to Córdoba University.

RNA Preparations

Total RNA was extracted from tissue by using the TRIzol reagent (Life Technologies) according to the manufacturer's protocol. Sample quality was checked electrophoretically, and quantification was done spectrophotometrically. Lack of DNA contamination was checked by PCR amplification of RNA samples without prior cDNA synthesis. The standard RNA was synthesized in vitro from a laboratory-engineered cDNA fragment containing a T7 polymerase binding site (Table 1), by means of a commercial RNA transcription kit (Stratagene). Commercial samples of total RNA were from Clontech, except those of ovary total RNA (mouse and human) from Ambion. RNA integrity and lack of DNA contamination were checked as outlined before. These RNAs were then quantified spectrophotometrically.

Quantitative Real-Time PCR

cDNA was generated from 2 μg of total RNA from each sample, using the M-MLV reverse transcriptase (Life Technologies) and random hexamers. The primer pairs used in this study are listed in Table 1. Primers were designed with Oligo 6.1.1/98 software (Molecular Biology Insights). To obtain the highest specificity, primers were chosen to have high T_m (≥84°C) and optimal 3′ ΔG (≥–8.7°C) values. Primers for *OGG1* were designed to amplify all known types of alternative transcripts (31). Primers for mouse and human transcripts were chosen to amplify homologous sequences. Real-time PCR reactions were performed at least in triplicate by using 50 ng of cDNA template, 0.3 μM of each primer (Table 1), 3 mM $MgCl_2$, 250 μM of each dNTP, 0.75 units of Platinum Taq DNA polymerase, and 1:100000 SYBR Green I dye (Roche) in a volume of 25 μl. Reactions were analyzed on an iCycler iQ Real-Time PCR System (BioRad). Cycling conditions were as follows: 2 min at 95°C for the Platinum Taq activation and 40 cycles for the melting (15 s, 95°C) and annealing/extension (30 s, 70°C) steps. These conditions generate specific PCR products of the desired length (Table 1). PCR products were further verified by nucleotide sequencing.

TABLE 1
PROPERTIES OF REVERSE TRANSCRIPTASE PCR AMPLICONS USED FOR ABSOLUTE QUANTITATION OF mRNA

Target	Length (bp)*	Primers†	Standard Curve Equation‡	Efficiency	Correlation Coefficient
mOGG1	159	5′-GCT GAG ACA AGA CCC CAC TGA GTG CCT TT-3′ (F) 5′-TGG AGG TTT GGG AAG CCA TGA TAA GTG ACA-3′ (R)	$y = -3.25x + 28.20$	1.03	0.99
hOGG1	103	5′-ACT GCT GCG ACA AGA CCC CAT CGA A-3′ (F) 5′-AGC CTG GCA CAG CCG CTC CAC-3′ (R)	$y = -3.33x + 27.30$	1.00	0.97
mAPE1	85	5′-CTT CCG GCA TCT CTA CCC CAA CAC TGC T-3′ (F) 5′-CCA ACC AAC ATT CTT AGA GCG GGC ATT CA-3′ (R)	$y = -3.32x + 28.07$	1.00	0.98
hAPE1	97	5′-GCC GGG TGA TTG TGG CTG AAT TTG A-3′ (F) 5′-CGC TGC CGG TAC TCC AGT CGT ACC A-3′ (R)	$y = -3.33x + 28.50$	1.00	0.98
mHO-1	121	5′-ATG CCC CAC TCT ACT TCC CTG AGG AGC TG-3′ (F) 5′-TAG TGC TGT GTG GCT GGC GTG CAA-3′ (R)	$y = -3.17x + 26.78$	1.07	0.99
hHO-1	123	5′-GCC CAG TCT TCG CCC CTG TCT ACT TCC-3′ (F) 5′-GCA TGG CTG GTG TGT AGG GGA TGA CC-3′ (R)	$y = -3.31x + 25.80$	1.00	0.99
mGAPD	137	5′-GGC TGC CCA GAA CAT CAT CCC TGC AT-3′ (F) 5′-ACG TCA GAT CCA CGA CGG ACA CAT TGG-3′ (R)	$y = -3.33x + 22.63$	1.00	0.98
hGAPD	138	5′-CGC GGG GCT CTC CAG AAC ATC ATC-3′ (F) 5′-CAG GTC CAC CAC TGA CAC GTT GGC A-3′ (R)	$y = -3.23x + 25.08$	1.04	0.99
mACTB	150	5′-GGC TGG CCG GGA CCT GAC AGA CTA C-3′ (F) 5′-GCA GTG GCC ATC TCC TGC TCG AAG TC-3′ (R)	$y = -3.23x + 18.83$	1.04	0.99
hACTB	151	5′-GGC TGG CCG GGA CCT GAC TGA CTA-3′ (F) 5′-AGC CGT GGC CAT CTC TTG CTC GAA G-3′ (R)	$y = -3.35x + 20.86$	0.99	1.00
External standard	130	5′-GGC TGC CCA GAA CAT CAT CCC TGC AT-3′ (F) 5′-ACG TCA GAT CCA CGA CGG ACA CAT TGG-3′ (R)	$y = -3.33x + 39.69$	1.00	1.00

*PCR product size (base pairs). The *mGAPD* gene and the external standard were amplified with the same pair primers, resulting in two PCR products: 137 bp from *mGAPD* and 130 bp from external standard (a laboratory engineered fragment with a 7-bp deletion).
†Sequence of forward (F) and reverse (R) primers.
‡Standard curve equations were obtained using lung samples, except those for *hOGG1* and *hHO-1* that were obtained using kidney samples.

The *mHO-1* primer pair in Table 1 amplified in *M. spretus* a single product exhibiting 100% DNA sequence identity with the known fragment in *M. musculus*. No primer dimers were present. Investigated transcripts showed optimal PCR efficiencies, in the range of 0.02–200 ng of total RNA input with high linearity (Table 1). An absolute standard curve was constructed with an external standard in the range of 10^9–10^2 RNA molecules. Separate cDNA synthesis reactions were undertaken with increasing amounts of RNA. The number of copies of the experimental transcripts was calculated from the linear regression of the standard curve (Table 1).

RESULTS

Determining Normal Variability in Mouse Gene Expression

Many factors, including the process of killing the animal, may contribute to mouse-to-mouse variability in gene expression (34). We initially faced this problem by isolating RNA from the liver of six genetically identical male BALB/c mice. The numbers of transcript molecules of *mOGG1, mAPE1*, and *mHO-1* were quantitated by real-time PCR in each of the liver samples (Table 2). Replicate reactions generated highly reproducible results with standard errors of <10% of the mean values (<1% for threshold cycle data). Interindividual variation was in the same range, demonstrating that those three genes have an outstanding stable expression among mice, in at least the liver. Based on these results, we assumed that the study would not be particularly vulnerable to misinterpretation due to natural differences in murine gene expression. Hence, the animal sample size was reduced in further assays.

Basal Expression Profiles in Mouse

The real-time analysis allowed us to examine accurately the basal expression levels of the three target genes (*mOGG1, mAPE1*, and *mHO-1*) and the two housekeeping genes (*mGAPDH* and *mACTB*) in all the organs examined (Fig. 1). Both low (less than 10^3 mRNA copies/ng of total RNA) and high (more than 10^6 copies/ng) basal expression levels were determined in a highly quantitative manner. For instance,

TABLE 2
VARIANCE IN MOUSE GENE EXPRESSION

	mOGG1		*mAPE1*		*mHO-1*	
Mouse	Molecules*	Mean ± SEM†	Molecules*	Mean ± SEM†	Molecules*	Mean ± SEM†
1	766		6097		3526	
	737		6307		4019	
	807	770 ± 20	5029	5811 ± 396	3901	3815 ± 149
2	—		4808		2955	
	666		4307		2927	
	733		5002		3850	
	672	690 ± 21	4581	4674 ± 150	3858	3398 ± 304
3	797		4706		3831	
	882		5772		4204	
	872	850 ± 27	6307	5595 ± 471	3516	3850 ± 199
4	643		4033		2731	
	620		3933		3955	
	782	682 ± 50	4885	4284 ± 302	3933	3540 ± 405
5	576		—		—	
	624		3874		2927	
	645		4358		2783	
	650	624 ± 17	3354	3862 ± 290	3320	3010 ± 161
6	—		5431		—	
	690		5984		3299	
	849		5820		3254	
	885	808 ± 60	5469	5676 ± 135	3536	3363 ± 87
Mean ± SEM‡		737 ± 35		4984 ± 336		3496 ± 128

*Transcript molecules per nanogram of total RNA from liver.
†Mean ± SEM of 3–4 PCR repetitions.
‡Mean ± SEM of 6 mice.

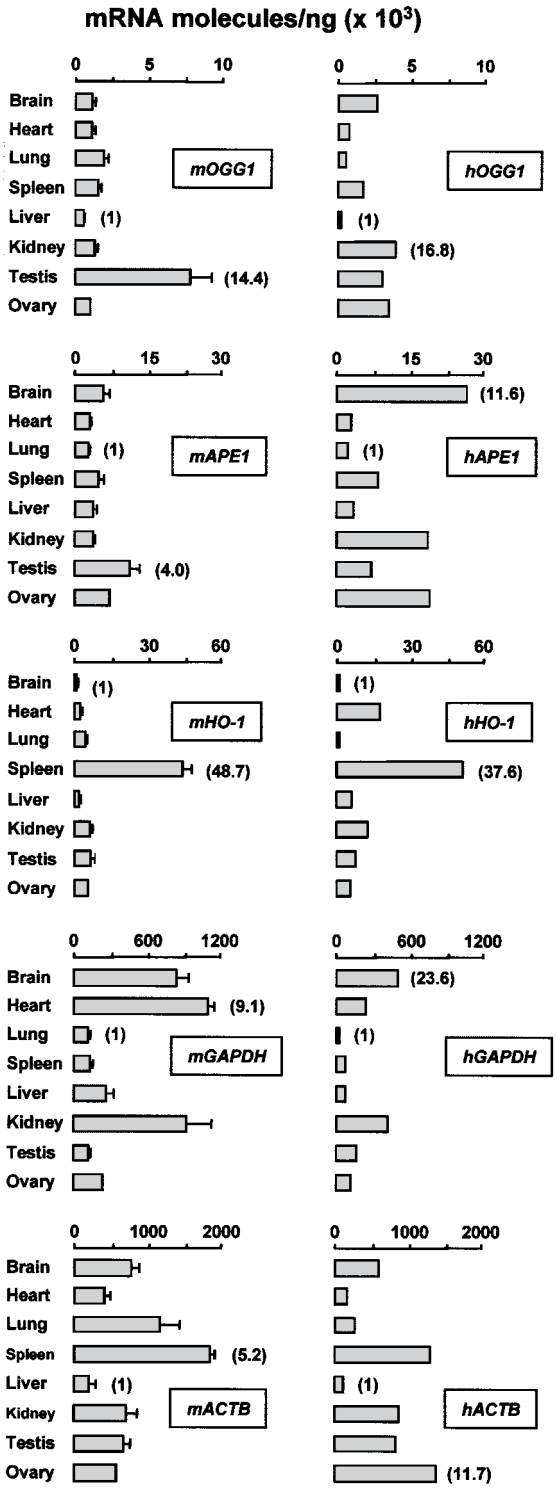

Figure 1. Organ-associated differences in basal levels of gene expression. The *x*-axis represents the average number of mRNA molecules per nanogram of total RNA. The *y*-axis represents each organ tested. Error bars indicate gene expression variability among three mice. Some error bars are not visible because of small SEM. No error bars are shown for mRNA quantitation of commercial samples (murine ovary and human organs). Variability among replicate PCR reactions did not exceed 10% of the mean. Maximal and minimal levels of basal expression were divided; the resulting fold variations are given in parentheses.

the number of *mACTB* transcripts in spleen (1840×10^3 molecules/ng) was 3400 times that of *mOGG1* in liver (543 molecules/ng). In agreement with data in Table 1, all the genes showed extraordinary consistency between identical samples from different mice. Hence, there was not more than twofold variation in gene expression between any two mice in the studied organs. Accordingly, no significant differences were found when data from individual organs (Table 1, Fig. 1) were compared with those achieved in commercial samples pooled from ≥100 mice (data not shown). Overall, the order of genes exhibiting the lowest to greatest amounts of basal levels of transcripts was *mOGG1* < *mAPE1* = *mHO-1* < *mGAPDH* < *mACTB*.

Although the three target genes were ubiquitously expressed, the copy number of each transcript varied depending on the tissue type (Fig. 1). We found that *mOGG1* was upregulated an average of 2.5-fold in brain, heart, lung, spleen, and kidney (at about 1370 transcript molecules/ng) compared with the liver level (543 molecules/ng). Nevertheless, a much higher upregulation of 14.4-fold (7824 molecules/ng) was found in testis. The *mAPE1* transcript was also particularly abundant in testis, although in this latter case maximal variation among the organs examined was less important (11223 molecules/ng in testis vs. 2786 molecules/ng in lung). This more homogeneous pattern of expression presumably is congruent with the multifunctional roles of APE1 (14).

Basal expression of *mHO-1* gene exhibited a strong spleen specificity [i.e., much higher number of transcripts (44110 molecules/ng) was quantitated in spleen than in the rest of the organs (<7000 molecules/ng)] (Fig. 1). Nevertheless, substantial differences among these other organs were also observed. Thus, *mHO-1* was upregulated an average of 7.2 in kidney and testis (at about 6500 molecules/ng) compared with the lowest level in brain (906 molecules/ng). In the line of the three target genes, vast differences in abundance of the two housekeeping transcripts (*mGAPDH* and *mACTB*) were quantitated among the various mouse tissues examined in this work.

Total RNAs from the eight major adult tissues in Figure 1 were then mixed at equal amounts to be used as the expression reference of differences associated to various stages of mouse embryonic development (Fig. 2). Genes were upregulated to different extent as a function of developmental age, and most genes exhibited maximal variations at the early fetal day 11. Of note is the large upregulation of *mAPE1* expression in the E11 (9.5-fold) and E15 (9.9-fold) embryos. Overall, embryos at the late fetal day 17 of gestation showed transcript levels quite similar to the mixture of RNAs from adult tissues. Recently, whole-

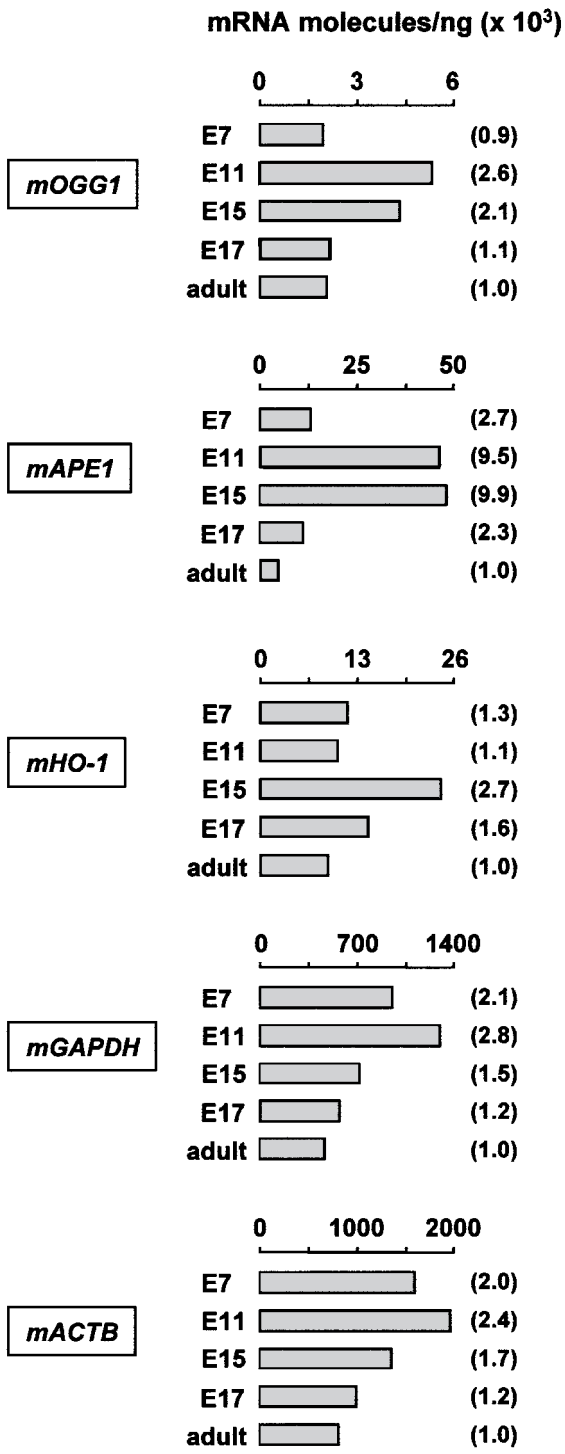

Figure 2. Embryo-associated differences in basal levels of gene expression. The *x*-axis represents the number of mRNA molecules per nanogram of total RNA. The *y*-axis indicates the embryonic day *n* (E*n*). Variability among replicate PCR reactions did not exceed 10% of the mean. According to the manufacturer's specifications, total RNA sources were normal whole embryos pooled from 200 mice. The numbers of mRNA molecules quantified in a mixture of total RNAs from the eight major adult tissues in Figure 1 are included as reference. The resulting fold variations are given in parentheses.

body cDNA from E17.5 embryos has been proposed as the reference material for comparison of microarray data between laboratories (30).

Association Between Basal Expression of Mouse and Human Genes

We wondered whether the murine expression patterns examined here were maintained in humans. We found similarities but also high differences between the human and murine expression levels for the different genes in a given organ (Fig. 1). For example, whereas the genes showed comparable expression levels in the spleen from both species (e.g., 51527 *hHO-1* vs. 44110 *mHO-1* transcript molecules/ng), basal expression levels in other human organs were much higher or lower than those quantitated in murine organs. Overall, we quantitated lower expression levels of the two DNA repair genes in human heart, lung, liver, and testis, but higher levels in human brain, kidney, and ovary compared with murine levels. Differences in basal expression levels between human and murine organs followed a different pattern for the transcripts that code for the HO-1 protein, where, for instance, much higher amounts were quantitated in heart from humans than from mice (17818 vs. 2477 transcripts/ng). Differences in the transcript levels for the two housekeeping genes were also evident; the human levels were generally lower than the murine levels.

Expression Profiles in Mouse Liver and Lung After PQ Treatment

Animals were challenged with PQ at 30 mg kg^{-1} body weight [approximately one half the LD_{50} (12)] in order to quantify the effect of this well-known generator of superoxide within cells on the mRNA abundance of *mOGG1, mAPE1*, and *mHO-1* genes. Time courses in liver and lung were analyzed (Fig. 3). The liver is often the target organ of toxic compounds; however, the lung is considered the primary target organ of PQ toxicity (a well-known pneumotoxicant). Control animals (saline IP) showed similar mRNA levels (Fig. 3) as those quantified in liver and lung from noninjected animals (Fig. 1); no time-related effect was noted (data not shown). In contrast, PQ generated specific gene induction profiles in both organs.

In liver, the 30 mg kg^{-1} IP injection of PQ upregulated the transcript levels of both *mAPE1* and *mHO-1* genes (Fig. 3). Upregulation exhibited biphasic profiles with minimal significant increments at 30 min and maximal induction factors of 2.1-fold (*mAPE1*) and 21.8-fold (*mHO-1*) at 120 min of PQ challenge. Thereafter, the amounts of *mAPE1* and *mHO-1* transcripts declined to basal levels within 240 min of

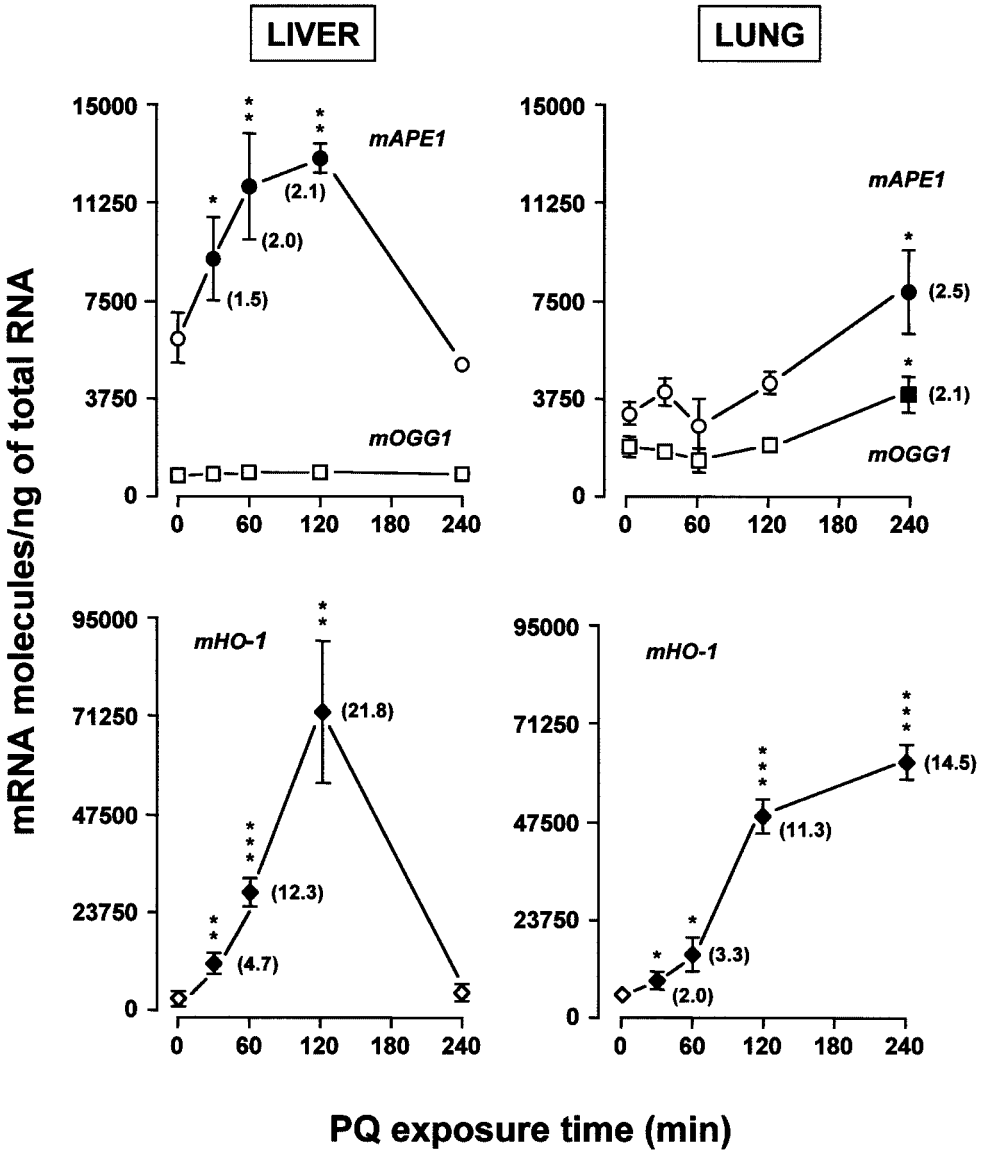

Figure 3. Time courses of liver and lung responses to PQ treatment. Control animals received a single IP injection of saline solution (NaCl 0.9%). Data presented at 0 min of PQ exposure are the mean values of transcript molecules per nanogram of total RNA ± SEM from five control mice. Treated animals received a single dose of PQ (30 mg kg^{-1} body weight). Data presented at 30, 60, 120, and 240 min of PQ exposure are the mean values of transcript molecules per nanogram of total RNA ± SEM from three mice. Some error bars are not visible because of small SEM. Statistical significance (*t*-test) is indicated by filled-in symbols and expressed as: $*p < 0.05$, $**p < 0.01$, and $***p < 0.001$. Increments relative to control mice are given in parentheses.

treatment. The *mOGG1* transcript level in liver did not respond to PQ at the exposure conditions tested in this work.

Whereas in liver the large upregulation of *mHO-1* expression in response to challenge posed by PQ was completely reversed at 240 min, the *mHO-1* transcript level in lung was significantly elevated at all time points to reach a maximal induction of 14.5-fold at 240 min of PQ exposure (Fig. 3). Concerning the lung expression of both DNA repair genes, the only effect toward significance was observed at the longer observation time of 240 min, with somewhat higher upregulation of *mAPE1* than *mOGG1* gene (2.5- vs. 2.1-fold increment in transcript molecules).

Animal Field Study

Interindividual variation is an indispensable information for a biomarker in epidemiological studies. It can be assumed that interindividual variation is genetically determined and epigenetically influenced by both endogenous and environmental reasons. We ex-

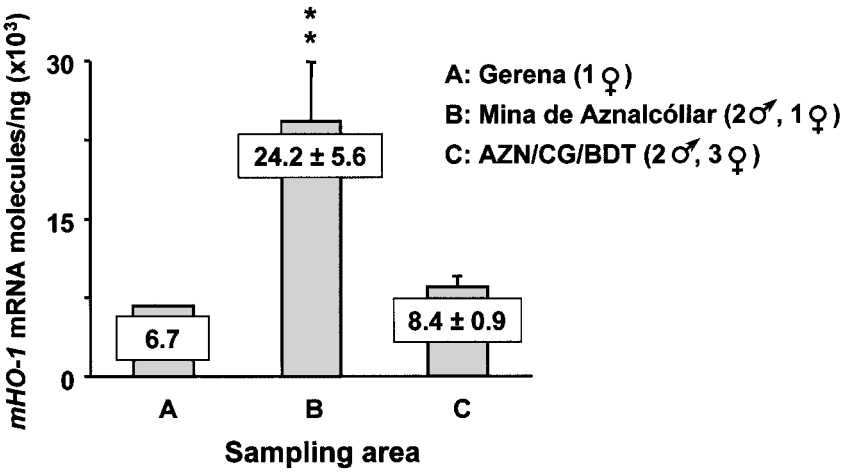

Figure 4. Sampling area-associated differences in *mHO-1* gene expression of Algerian mouse. Sampling areas are given in the *x*-axis. The *y*-axis represents the average number of mRNA molecules per nanogram of total RNA from liver. Error bars indicate gene expression variability among the three (B) or five (C) captured mice. Statistical significance (**$p < 0.01$) with respect to sampling area C was determined by the Student's *t*-test.

amined this problem by quantitating the *mHO-1* transcript levels in the liver from genetically diverse animals.

Algerian mouse (*Mus spretus*) is a nonprotected and free-living species that has been used as sentinel organism (bioindicator) to assess the effects of environmental pollution caused by the Aznalcóllar mining spill (38). Figure 4 shows the numbers of *mHO-1* transcripts quantified in the liver of nine Algerian mice collected 3 years and 7 months after the Aznalcóllar disaster at five different sampling areas (38). The *mHO-1* mRNA levels yielded a clear geographic discrimination: animals from Mina de Aznalcóllar had levels 2.9-fold higher than those captured at the three downstream Guadiamar areas (AZN, CG, and BDT). This result is in agreement with the idea that Mina de Aznalcóllar (the area closer to the collapsed dam) represents the sampling zone most heavily polluted with pyrite-related metals. In comparison, as indicated by several biochemical biomarkers (25), the three areas along the Guadiamar river course, although initially affected by the Aznalcóllar spill, are at present returning to normal control levels. Indeed, as shown in Figure 4, animals from these three zones had *mHO-1* transcript levels similar to that from the single female mouse captured in Gerena, an upstream reference area considered free of contaminants.

DISCUSSION

Real-time PCR is becoming increasingly popular in the study of gene expression. Most published articles utilizing real-time PCR report the magnitude of relative expression differences among samples to be compared. The main drawback of this method is the unproven existence of internal control genes (24). Therefore, large errors in the derived estimates of fold change in the expression of target genes can be yielded (17). In this study we avoid determining appropriate endogenous control genes by absolute quantitation of mRNAs levels.

In vivo studies on gene expression profiles are relatively uncommon and in particular no data have been reported concerning the absolute transcript abundance of several genes in different mammalian organs. Two of the genes (encoding GAPDH and β-actin) chosen for this study are among the most popular internal controls used to normalize RNA levels in Northern hybridization analysis, ribonuclease protection, or RT-PCR (42). We demonstrate by absolute quantitation that transcript levels of these two genes, from either murine or human origin, fluctuate dramatically across diverse biological tissues: maximal fold change ranged from 5.2 for *mACTB* to 23.6 for *hGAPDH*. Clearly, this finding raises the question about the inaccuracy of using these genes as internal standards to analyze tissue-specific mRNA profiling. Likewise, it is also apparent that *GADPH* and *ACTB* genes do not serve as control genes for studies performed in a single tissue context because there is widespread evidence showing that the transcription levels of mammalian *GADPH* and *ACTB* vary significantly in response to different experimental manipulations (7).

Previous studies based on Northern blot, and commonly using *ACTB* or *GAPDH* as reference gene, have examined basal levels of *OGG1* or *APE1* mRNA in a variety of murine (mouse or rat) and human tissues

(2,3,35,37,43,44,48). Overall, these analyses gave very poor signals and data generated are controversial and hardly conclusive, except for the impression of a nearly ubiquitous transcription. The real-time PCR analysis performed here revealed those mouse genes (*mOGG1* and *mAPE1*) coding for DNA repair enzymes as being preferentially expressed in testis and quantified for the first time this testis-specific expression pattern. Elevated expression in adult mouse testis of genes coding for base excision repair proteins have been explained by the need to minimize germ-line mutations (22). Of note, however, is that no testis-preferential expression was detected in human samples, thus suggesting potential important differences among mammalian species to this respect. Nevertheless, both *hOGG1* and *hAPE1* transcripts were present at greater amounts in testis than in other human organs, like heart, lung or liver.

Both *mOGG1* and *mAPE1* also showed elevated expressions in 11- and 15-day mouse embryos, suggesting that they could provide protection against DNA damage during fetal development. Interestingly, the large upregulation of *mAPE1* at the early fetal day 11 seems in agreement with a recent study showing that null APE1 embryos exhibit successful implantation and nearly normal development progression until day 7.5, followed by morphogenetic failure and absorption of embryos by day 9.5 (27).

Despite intense investigation into HO-1, a systematic and quantitative examination on the *HO-1* mRNA abundance among different mouse or human tissues remains largely undetermined. Here we quantified an outstanding spleen-specific expression pattern in both species, in agreement with the observation that in rat spleen HO-1 is the predominant isoform (5) and likely because of a constant exposure to hemoglobin released in the course of disruption of senescent erythrocytes. Nonetheless, relatively large amounts of *HO-1* transcripts were also quantitated in other mouse and human organs like testis (i.e., 6858 and 7785 molecules/ng for *mHO-1* and *hHO-1*, respectively) where HO-2 is commonly viewed as the predominant variant (15,45,46).

Induction of *OGG1* mRNA in cultured cells under severe oxidative stress conditions is highly controversial (11,29,40). Similarly, although the amounts of *APE1* mRNA and protein were shown to increase in cells treated for 6–9 h with a variety of ROS generators, like hypochlorous acid, H_2O_2, and γ-rays (16,36), there is also one report on the absence of such in vitro activation after treatment with PQ and other DNA-damaging agents (18). On the other hand, few in vivo studies have reported the induction of *OGG1* or *APE-1* gene in response to oxidative stress caused by long-term treatments with diesel exhaust particles (environmental pollutant), phenobarbital (liver tumor promoter), or WY-14,643 (peroxisome proliferator) (23, 39,47).

Historically, heme oxygenase was one of the first enzymes shown to be upregulated by oxidants. In vitro and in vivo studies have reported increments in both the protein and the transcription of *HO-1* gene in response to treatments able to generate oxidative stress in cells and tissues (1,4,8,32). However, PQ (a model superoxide generator) is not included in the list of typical *HO-1* stressors (20,28,33). In short, to our knowledge, no previous reports have described any change in *OGG1*, *APE1,* or *HO-1* mRNA levels associated with superoxide stress in experimental animals and have precisely quantitated such a response thus far.

In the current in vivo study we demonstrated significant differences between control and PQ-treated animals, with reproducible and coordinated variations as a function of exposure time and organ for all target genes investigated. The important finding that PQ at 30 mg kg^{-1} (IP) upregulates the in vivo levels of *mOGG1*, *mAPE1,* and *mHO-1* transcripts provides further support for a role for these genes in protection against oxidative stress. Our study demonstrates that both liver and lung are readily responding during the 30–240 min following exposure to PQ at a moderate dose of one half the documented LD_{50} value (12). Additionally, data reported suggest that the rapid reversal of the liver response (compared to lung) might be the logical result of a quick and outstanding in vivo induction of genes (like *HO-1*) that may serve as a primary line of cellular defense. Our data do not discriminate whether PQ increased gene expression in both liver and lung cells per se or via other effector cells (e.g., macrophages in an inflammatory response) within the organs examined. However, this second possibility is unlikely because no inflammatory response has been detected (e.g., in lung tissue) on histopathological analysis of wild-type mice at 240 min after identical PQ challenge (10).

Overall, both DNA repair genes (*mOGG1* and *mAPE1*) showed similar murine expression patterns with high basal transcript levels in testis and moderate, but significant, responses to superoxide stress. Recent data suggest coordinated functions of OGG1 and APE1, and possible other enzymes, in the DNA base excision repair pathway (19,40). It can be hypothesized that genes in the same pathway leading to a particular expression pattern would correlate more highly among themselves than with the other genes.

On April 25, 1998, a tailing dam of the Aznalcóllar pyrite mine partially collapsed and released to the Guadiamar river acid water and mud containing toxic metals, threatening the Doñana National Park, a Span-

ish wildlife reserve. Removal of contaminated mud started in May and was nearly completed by October 1998. Several biochemical parameters have been used as pollution biomarkers in Algerian mouse liver to monitor possible biological effects in terrestrial ecosystems of the Aznalcóllar disaster (38). Data reported here assayed for the first time the utility of absolute quantitation of transcript levels of stress-responsive genes (like *mHO-1*) in sentinel organisms (like *M. spretus*) as biomarkers of environmental pollution. We show that the number of *mHO-1* mRNA molecules in mouse liver discriminates an area (Mina de Aznalcóllar) heavily polluted with prooxidant metals (like Fe, As, Cu, and Cd) from three downstream areas (AZN, CG, and BDT) of the Guadiamar course affected by spilt metals, at about 3 years after the mud removal.

Taken together, data reported here conclusively establish that real-time PCR is a highly sensitive and reproducible technique for absolute quantitation of transcript levels in vivo. Because additionally this technique requires small amounts of starting RNA, we reasoned that such quantitative measurements would be particularly suitable for modulation of gene expression under physiological exposures and for epidemiological studies. Data in the Algerian mouse, a common free-living rodent, represent a challenge for further studies of human gene expression and for developing diagnostic biomarkers for diseases, including cancer. Finally, to remark that although absolute quantitation of transcript levels does not allow knowledge on protein activity, a hallmark of most molecular pathways, the experimental approach used here would allow the identification of transcriptional target of these pathways.

ACKNOWLEDGMENTS

M.J.P.-A. was recipient of a postdoctoral contract and J.M.C.-L. of a predoctoral fellowship from the Ministerio de Educación y Cultura. This work was supported by Grants PB98-1627 and BMC2002-00179.

REFERENCES

1. Abe, T.; Yamamoto, O.; Gotoh, S.; Yan, Y.; Todaka, N.; Higashi, K. Cadmium-induced mRNA expression of Hsp32 is augmented in metallothionein-I and -II knock-out mice. Arch. Biochem. Biophys. 382:81–88; 2000.
2. Aburatani, H.; Hippo, Y.; Ishida, T.; Takashima, R.; Matsuba, C.; Kodama, T.; Takao, M.; Yasui, A.; Yamamoto, K.; Asano, M. Cloning and characterization of mammalian 8-hydroxyguanine-specific DNA glycosylase/apurinic, apyrimidinic lyase, a functional mutM homologue. Cancer Res. 57:2151–2156; 1997.
3. Akiyama, K.; Seki, S.; Oshida, T.; Yoshida, M. C. Structure, promoter analysis and chromosomal assignment of the human APEX gene. Biochim. Biophys. Acta 1219:15–25; 1994.
4. Applegate, L. A.; Luscher, P.; Tyrrell, R. M. Induction of heme oxygenase: A general response to oxidant stress in cultured mammalian cells. Cancer Res. 51: 974–978; 1991.
5. Braggins, P. E.; Trakshel, G. M.; Kutty, R. K.; Maines, M. D. Characterization of two heme oxygenase isoforms in rat spleen: Comparison with the hematin-induced and constitutive isoforms of the liver. Biochem. Biophys. Res. Commun. 141:528–533; 1986.
6. Bruner, S. D.; Norman, D. P.; Verdine, G. L. Structural basis for recognition and repair of the endogenous mutagen 8-oxoguanine in DNA. Nature 403:859–866; 2000.
7. Bustin, S. A. Absolute quantification of mRNA using real-time reverse transcription polymerase chain reaction assays. J. Mol. Endocrinol. 25:169–193; 2000.
8. Cho, H. Y.; Jedlicka, A. E.; Reddy, S. P.; Kensler, T. W.; Yamamoto, M.; Zhang, L. Y.; Kleeberger, S. R. Role of NRF2 in protection against hyperoxic lung injury in mice. Am. J. Respir. Cell. Mol. Biol. 26: 175–182; 2002.
9. Davies, K. J. Oxidative stress, antioxidant defenses, and damage removal, repair, and replacement systems. IUBMB Life 50:279–289; 2000.
10. de Haan, J. B.; Bladier, C.; Griffiths, P.; Kelner, M.; O'Shea, R. D.; Cheung, N. S.; Bronson, R. T.; Silvestro, M. J.; Wild, S.; Zheng, S. S.; Beart, P. M.; Hertzog, P. J.; Kola, I. Mice with a homozygous null mutation for the most abundant glutathione peroxidase, Gpx1, show increased susceptibility to the oxidative stress- inducing agents paraquat and hydrogen peroxide. J. Biol. Chem. 273:22528–22536; 1998.
11. Dhenaut, A.; Boiteux, S.; Radicella, J. P. Characterization of the *hOGG1* promoter and its expression during the cell cycle. Mutat. Res. 461:109–118; 2000.
12. Drew, R.; Gram, T. E. Vehicle alteration of paraquat lethality in mice. Toxicol. Appl. Pharmacol. 48:479–487; 1979.
13. Elder, P. K.; French, C. L.; Subramaniam, M.; Schmidt, L. J.; Getz, M. J. Evidence that the functional beta-actin gene is single copy in most mice and is associated with 5′ sequences capable of conferring serum- and cycloheximide-dependent regulation. Mol. Cell. Biol. 8:480–485; 1988.
14. Evans, A. R.; Limp-Foster, M.; Kelley, M. R. Going APE over ref-1. Mutat. Res. 461:83–108; 2000.
15. Gibbs, L.; Willis, D.; Morgan, M. J. The identification and expression of heme oxygenase-2 alternative transcripts in the mouse. Gene 221:171–177; 1998.
16. Grosch, S.; Fritz, G.; Kaina, B. Apurinic endonuclease (Ref-1) is induced in mammalian cells by oxidative stress and involved in clastogenic adaptation. Cancer Res. 58:4410–4416; 1998.

17. Hanaoka, T.; Yamano, Y.; Hashimoto, H.; Kagawa, J.; Tsugane, S. A preliminary evaluation of intra- and interindividual variations of *hOGG1* messenger RNA levels in peripheral blood cells as determined by a real-time polymerase chain reaction technique. Cancer Epidemiol. Biomarkers Prev. 9:1255–1258; 2000.
18. Harrison, L.; Ascione, A. G.; Wilson, D. M., 3rd; Demple, B. Characterization of the promoter region of the human apurinic endonuclease gene (APE). J. Biol. Chem. 270:5556–5564; 1995.
19. Hill, J. W.; Hazra, T. K.; Izumi, T.; Mitra, S. Stimulation of human 8-oxoguanine-DNA glycosylase by AP-endonuclease: Potential coordination of the initial steps in base excision repair. Nucleic Acids Res. 29:430–438; 2001.
20. Hill-Kapturczak, N.; Chang, S. H.; Agarwal, A. Heme oxygenase and the kidney. DNA Cell Biol. 21:307–321; 2002.
21. Hough, C. D.; Cho, K. R.; Zonderman, A. B.; Schwartz, D. R.; Morin, P. J. Coordinately up-regulated genes in ovarian cancer. Cancer Res. 61:3869–3876; 2001.
22. Intano, G. W.; McMahan, C. A.; Walter, R. B.; McCarrey, J. R.; Walter, C. A. Mixed spermatogenic germ cell nuclear extracts exhibit high base excision repair activity. Nucleic Acids Res. 29:1366–1372; 2001.
23. Kinoshita, A.; Wanibuchi, H.; Imaoka, S.; Ogawa, M.; Masuda, C.; Morimura, K.; Funae, Y.; Fukushima, S. Formation of 8-hydroxydeoxyguanosine and cell-cycle arrest in the rat liver via generation of oxidative stress by phenobarbital: Association with expression profiles of $p21^{WAF1/Cip1}$, cyclin D1 and Ogg1. Carcinogenesis 23: 341–349; 2002.
24. Lee, P. D.; Sladek, R.; Greenwood, C. M.; Hudson, T. J. Control genes and variability: Absence of ubiquitous reference transcripts in diverse mammalian expression studies. Genome Res. 12:292–297; 2002.
25. López-Barea, J.; Ruíz-Laguna, J.; Bonilla, D.; Muñoz, A.; Moreno, S. Biochemical biomarkers of pollution in Algerian mouse (*Mus spretus*) to assess the biological effects of Aznalcóllar mining spill. In: Delvalls, T. A.; Blasco, J., eds. Integrated assessment and management of the ecosystems affected by the Aznalcóllar mining spill (SW, Spain). IOC/ICAM/UNESCO Technical report (in press).
26. Lu, R.; Nash, H. M.; Verdine, G. L. A mammalian DNA repair enzyme that excises oxidatively damaged guanines maps to a locus frequently lost in lung cancer. Curr. Biol. 7:397–407; 1997.
27. Ludwig, D. L.; MacInnes, M. A.; Takiguchi, Y.; Purtymun, P. E.; Henrie, M.; Flannery, M.; Meneses, J.; Pedersen, R. A.; Chen, D. J. A murine AP-endonuclease gene-targeted deficiency with post-implantation embryonic progression and ionizing radiation sensitivity. Mutat. Res. 409:17–29; 1998.
28. Maines, M. D. Heme oxygenase: Function, multiplicity, regulatory mechanisms, and clinical applications. FASEB J. 2:2557–2568; 1988.
29. Merrill, C. L.; Ni, H.; Yoon, L. W.; Tirmenstein, M. A.; Narayanan, P.; Benavides, G. R.; Easton, M. J.; Creech, D. R.; Hu, C. X.; McFarland, D. C.; Hahn, L. M.; Thomas, H. C.; Morgan, K. T. Etomoxir-induced oxidative stress in HepG2 cells detected by differential gene expression is confirmed biochemically. Toxicol. Sci. 68:93–101; 2002.
30. Miki, R.; Kadota, K.; Bono, H.; Mizuno, Y.; Tomaru, Y.; Carninci, P.; Itoh, M.; Shibata, K.; Kawai, J.; Konno, H.; Watanabe, S.; Sato, K.; Tokusumi, Y.; Kikuchi, N.; Ishii, Y.; Hamaguchi, Y.; Nishizuka, I.; Goto, H.; Nitanda, H.; Satomi, S.; Yoshiki, A.; Kusakabe, M.; DeRisi, J. L.; Eisen, M. B.; Iyer, V. R.; Brown, P. O.; Muramatsu, M.; Shimada, H.; Okazaki, Y.; Hayashizaki, Y. Delineating developmental and metabolic pathways in vivo by expression profiling using the RIKEN set of 18,816 full-length enriched mouse cDNA arrays. Proc. Natl. Acad. Sci. USA 98: 2199–2204; 2001.
31. Nishioka, K.; Ohtsubo, T.; Oda, H.; Fujiwara, T.; Kang, D.; Sugimachi, K.; Nakabeppu, Y. Expression and differential intracellular localization of two major forms of human 8-oxoguanine DNA glycosylase encoded by alternatively spliced OGG1 mRNAs. Mol. Biol. Cell. 10:1637–1652; 1999.
32. Oshiro, S.; Takeuchi, H.; Matsumoto, M.; Kurata, S. Transcriptional activation of heme oxygenase-1 gene in mouse spleen, liver and kidney cells after treatment with lipopolysaccharide or hemoglobin. Cell Biol. Int. 23:465–474; 1999.
33. Otterbein, L. E.; Choi, A. M. Heme oxygenase: Colors of defense against cellular stress. Am. J. Physiol. Lung Cell. Mol. Physiol. 279:L1029–L1037; 2000.
34. Pritchard, C. C.; Hsu, L.; Delrow, J.; Nelson, P. S. Project normal: Defining normal variance in mouse gene expression. Proc. Natl. Acad. Sci. USA 98:13266–13271; 2001.
35. Radicella, J. P.; Dherin, C.; Desmaze, C.; Fox, M. S.; Boiteux, S. Cloning and characterization of *hOGG1*, a human homolog of the *OGG1* gene of *Saccharomyces cerevisiae*. Proc. Natl. Acad. Sci. USA 94:8010–8015; 1997.
36. Ramana, C. V.; Boldogh, I.; Izumi, T.; Mitra, S. Activation of apurinic/apyrimidinic endonuclease in human cells by reactive oxygen species and its correlation with their adaptive response to genotoxicity of free radicals. Proc. Natl. Acad. Sci. USA 95:5061–5066; 1998.
37. Rosenquist, T. A.; Zharkov, D. O.; Grollman, A. P. Cloning and characterization of a mammalian 8-oxoguanine DNA glycosylase. Proc. Natl. Acad. Sci. USA 94:7429–7434; 1997.
38. Ruíz-Laguna, J.; García-Alfonso, C.; Peinado, J.; Moreno, S.; Ieradi, L. A.; Cristaldi, M.; López-Barea, J. Biochemical biomarkers of pollution in Algerian mouse (*Mus spretus*) to assess the effects of the Aznalcóllar disaster on Doñana Park (Spain). Biomarkers 6:146–160; 2001.
39. Rusyn, I.; Denissenko, M. F.; Wong, V. A.; Butterworth, B. E.; Cunningham, M. L.; Upton, P. B.; Thurman, R. G.; Swenberg, J. A. Expression of base excision repair enzymes in rat and mouse liver is induced by peroxisome proliferators and is dependent upon carcinogenic potency. Carcinogenesis 21:2141–2145; 2000.

40. Saitoh, T.; Shinmura, K.; Yamaguchi, S.; Tani, M.; Seki, S.; Murakami, H.; Nojima, Y.; Yokota, J. Enhancement of OGG1 protein AP lyase activity by increase of APEX protein. Mutat. Res. 486:31–40; 2001.
41. Schmidt, E. E.; Merrill, G. F. Changes in dihydrofolate reductase (DHFR) mRNA levels can account fully for changes in DHFR synthesis rates during terminal differentiation in a highly amplified myogenic cell line. Mol. Cell. Biol. 11:3726–3734; 1991.
42. Suzuki, T.; Higgins, P. J.; Crawford, D. R. Control selection for RNA quantitation. Biotechniques 29:332–337; 2000.
43. Tan, Y.; Nakagawa, Y.; Akiyama, K.; Wakabayashi, H.; Sarker, A. H.; Seki, S. cDNA cloning of rat major AP endonuclease (APEX nuclease) and analyses of its mRNA expression in rat tissues. Acta Med. Okayama 50:53–60; 1996.
44. Tani, M.; Shinmura, K.; Kohno, T.; Shiroishi, T.; Wakana, S.; Kim, S. R.; Nohmi, T.; Kasai, H.; Takenoshita, S.; Nagamachi, Y.; Yokota, J. Genomic structure and chromosomal localization of the mouse Ogg1 gene that is involved in the repair of 8-hydroxyguanine in DNA damage. Mamm. Genome 9:32–37; 1998.
45. Trakshel, G. M.; Kutty, R. K.; Maines, M. D. Purification and characterization of the major constitutive form of testicular heme oxygenase. The noninducible isoform. J. Biol. Chem. 261:11131–11137; 1986.
46. Trakshel, G. M.; Maines, M. D. Detection of two heme oxygenase isoforms in the human testis. Biochem. Biophys. Res. Commun. 154:285–291; 1988.
47. Tsurudome, Y.; Hirano, T.; Yamato, H.; Tanaka, I.; Sagai, M.; Hirano, H.; Nagata, N.; Itoh, H.; Kasai, H. Changes in levels of 8-hydroxyguanine in DNA, its repair and OGG1 mRNA in rat lungs after intratracheal administration of diesel exhaust particles. Carcinogenesis 20:1573–1576; 1999.
48. Wilson, T. M.; Rivkees, S. A.; Deutsch, W. A.; Kelley, M. R. Differential expression of the apurinic/apyrimidinic endonuclease (APE/ref-1) multifunctional DNA base excision repair gene during fetal development and in adult rat brain and testis. Mutat. Res. 362:237–248; 1996.
49. Yoshikawa, T.; Toyokuni, S.; Yamamoto, Y.; Naito, Y., eds. Free radicals in chemistry, biology and medicine. London: OICA International (UK) Limited; 2000.